

Supplement informations

Redox reaction in two-dimensional porous coordination polymers based on ferrocenedicarboxylates

Kenji Hirai,^a Hiromitsu Uehara,^b Susumu Kitagawa*^{a,b,c} and Shuhei Furukawa*^{b,c}

^a *Department of Synthetic Chemistry and Biological Chemistry, Graduate School of Engineering, Kyoto University, Katsura, Nishikyo-ku, Kyoto 615-8510, Japan.*

^b *ERATO Kitagawa Integrated Pores Project, Japan Science and Technology Agency (JST), Kyoto Research Park bldg #3, Shimogyo-ku, Kyoto 600-8815, Japan. Fax: +81-75-322-4711; Tel: +81-75-325-3572;*

^c *Institute for Integrated Cell-Material Sciences, Kyoto University, Yoshida, Sakyo-ku, Kyoto 606-8501, Japan*

Contents

1. Experimental Section
2. Pore Structures of **1**
3. Pore Structures of **2**
4. Pore Structures of **3**
5. Thermogravimetric analysis of **1**, **2** and **3**
6. XRD of bulk powder crystals of **1**
7. XRD of bulk powder crystals of **2**
8. XRD of bulk powder crystals of **3**
9. Adsorption measurement of **1**
10. Adsorption measurement of **2**
11. Adsorption measurement of **3**
12. XRD of Crystals of **2** on Au electrodes
13. XRD of Crystals of **3** on Au electrodes
14. IR-RAS measurement of Crystals of **1** on an Au electrode

1. Experimental Section

Materials

Zn(NO₃)₂•6H₂O, 1,1'-ferrocenedicarboxylic acid (H₂Fcdc), 1,4-diaza[2.2.2]bicyclooctane (dabco), 4,4'-bipyridyl (bpy), *N,N'*-dimethylformamide (DMF) and methanol (MeOH) were purchased from Wako Pure Chemical Industries. The syntheses of 1,4-di(pyridin-4-yl)benzene (dpb) and *N,N'*-di(4-pyridyl)-1,4,5,8-naphthalenetetracarboxydiimide (dpndi), were prepared according to literature procedures^{S1, S2}.

Synthesis of 1

The solution of Zn(NO₃)₂•6H₂O (84.8 mg, 0.286 mmol), H₂Fcdc (78.3 mg, 0.286 mmol), and bpy (44.8 mg, 0.286 mmol) in 10 mL DMF/MeOH (DMF : MeOH = 2 : 1) were heated up to 353 K for 2 days. After cooling, the crystals were harvested. Elemental analysis calcd. for C₂₄H_{21.5}N_{2.5}O₅ZnFe {[Zn(Fcdc)(bpy)]•(DMF)_{0.5}(MeOH)_{0.5}}_n: C, 52.78; H, 3.97; N, 6.41, Found: C, 49.58; H, 3.73; N, 6.28.

Synthesis of 2

The solution of Zn(NO₃)₂•6H₂O (74.3 mg, 0.25 mmol), H₂Fcdc (68.5 mg, 0.25 mmol), and dpb (58.0 mg, 0.25 mmol) in 10 mL DMF/MeOH (DMF : MeOH = 1 : 2) were heated up to 373 K for 2 days. After cooling, the crystals were harvested. Elemental analysis calcd. for C₃₀H_{25.5}N_{2.5}O₅ZnFe {[Zn(Fcdc)(dpb)]•(DMF)_{0.5}(MeOH)_{0.5}}_n: C, 57.91; H, 4.13; N, 5.63, Found: C, 53.22; H, 3.77; N, 5.09.

Synthesis of 3

The solution of Zn(NO₃)₂•6H₂O (74.3 mg, 0.25 mmol), H₂Fcdc (68.5 mg, 0.25 mmol), and dpndi (105 mg, 0.25 mmol) in 10 mL DMF/MeOH (DMF : MeOH = 2 : 1) were heated up to 353 K for 2 days. After cooling, the crystals were harvested. Elemental analysis calcd. for C₃₈H_{37.5}N_{4.5}O₉ZnFe {[Zn(Fcdc)(dpndi)]•(DMF)_{0.5}(MeOH)_{0.5}}_n: C, 55.49; H, 4.60; N, 7.66, Found: C, 54.56; H, 3.30; N, 7.89.

Fabrication of 1 on Au substrates

The stocked reaction solution of 1 was prepared as Zn(NO₃)₂•6H₂O (84.8 mg, 0.286 mmol), H₂Fcdc (78.3 mg, 0.286 mmol), and bpy (44.8 mg, 0.286 mmol) in the mixed solvent (6.7 mL of DMF and 3.3 mL of MeOH). A gold substrate was placed in the solution and the reaction mixture was heated up to 353 K for 4 days. After cooling, the wafers were rinsed with DMF.

Fabrication of 2 on Au substrates

The stocked reaction solution of **2** was prepared as $\text{Zn}(\text{NO}_3)_2 \cdot 6\text{H}_2\text{O}$ (14.9 mg, 0.05 mmol), H_2Fcdc (13.7 mg, 0.05 mmol), and dpb (11.6 mg, 0.05 mmol) in the mixed solvent (3.3 mL of DMF and 6.7 mL of MeOH). A gold substrate was placed in the solution and the reaction mixture was heated up to 373 K for 4 days. After cooling, the wafers were rinsed with DMF.

Fabrication of 3 on Au substrates

The stocked reaction solution of **3** was prepared as $\text{Zn}(\text{NO}_3)_2 \cdot 6\text{H}_2\text{O}$ (74.3 mg, 0.25 mmol), H_2Fcdc (68.5 mg, 0.25 mmol), and dpndi (105 mg, 0.25 mmol) in the mixed solvent (6.7 mL of DMF and 3.3 mL of MeOH). A gold substrate was placed in the solution and the reaction mixture was heated up to 353 K for 4 days. After cooling, the wafers were rinsed with DMF.

Characterization methods

The PCP crystals were characterized with X-ray diffraction (XRD), thermogravimetry (TG), elemental analysis and IR-RAS. Powder X-Ray diffraction (XRD) studies were measured using a Rigaku diffractometer with $\text{Cu K}\alpha$ radiation ($\lambda = 1.5418 \text{ \AA}$). Surface XRD diffraction (SXRD) studies were measured using Rigaku SmartLab ($\lambda = 1.5418 \text{ \AA}$). TG measurements were carried out by Thermo plus EVO II. Elemental analysis was carried out on a Flash EA 1112 series, Thermo Finnigan instrument. Single crystal X-ray diffraction measurements were made on a Rigaku AFC10 diffractometer with Rigaku Saturn CCD system equipped with a rotating-anode X-ray generator producing multi-layer mirror monochromated $\text{MoK}\alpha$ radiation. IR-RAS measurement was performed by JASCO FT-IR6100.

Physical measurements

Gas sorption isotherms of N_2 , O_2 and CO_2 were recorded on a BELSORP-mini volumetric-adsorption instrument from BEL Japan. Cyclic voltammetry (CV) studies were carried out with an ALS400B electrochemical analyzer utilizing the three-electrode configuration of an Au substrate electrode, a Pt auxiliary electrode and a Ag/AgCl reference electrode. The measurements were performed in CH_2Cl_2 solution containing tetrabutylammonium tetrafluoroborate or tetrabutylammonium nitrate (0.1 mol L^{-1}) as supporting electrolyte. CV curves were recorded at various scan rates.

Structural determinationPhysical measurements

X-ray data collection ($5^\circ < 2\theta < 55^\circ$) was conducted at 223K on Rigaku AFC10 diffractometer $\text{Mo-K}\alpha$ radiation ($\lambda = 0.7105 \text{ \AA}$) with Rigaku Saturn CCD system. The structures were solved by a direct method (SIR92) and expanded using Fourier techniques. All calculations were performed using the CrystalStructure crystallographic software package 4.0 of Rigaku. These data can be obtained free of charge from The Cambridge Crystallographic Data Centre via www.ccdc.cam.ac.uk/data_request/cif.

2. Pore Structures of **1**

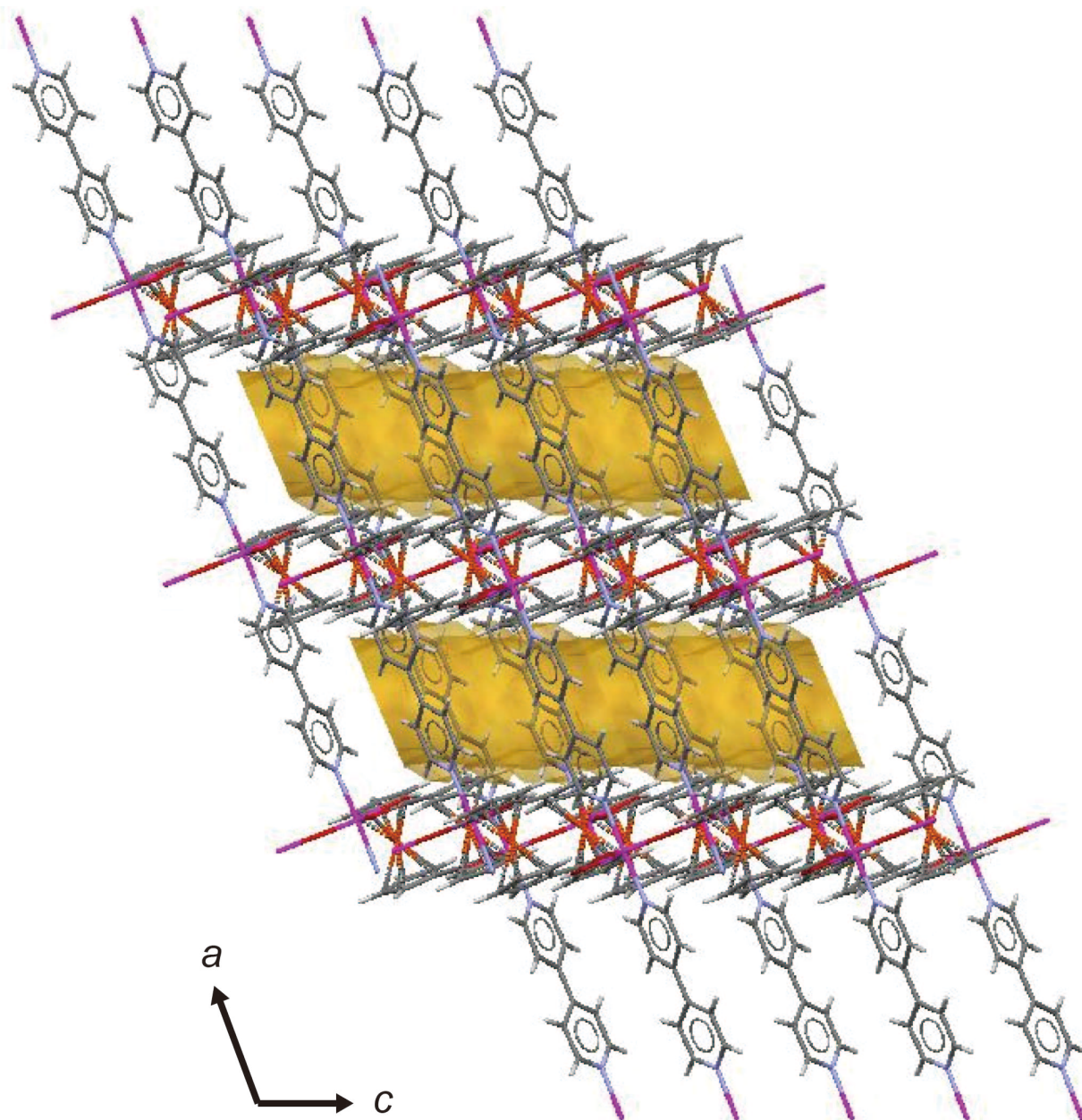


Fig. S1 Contact surface with a probe radius of 1.2 Å emphasizing the undulating 1D channels (gold) of **1**.

3. Pore Structures of 2

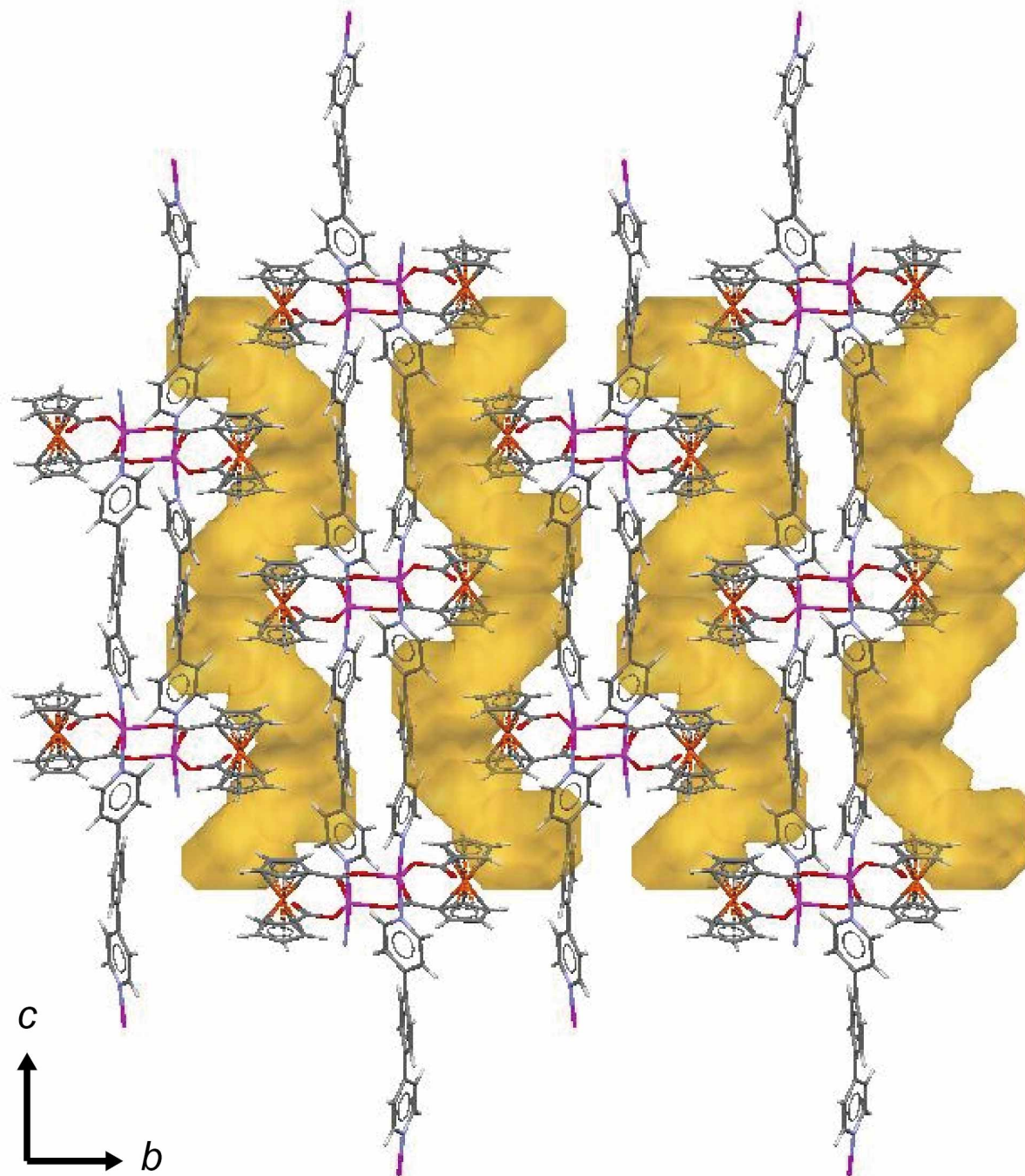


Fig. S2 Contact surface with a probe radius of 1.2 Å emphasizing the undulating 1D channels (gold) of 2.

4. Pore Structures of **3**

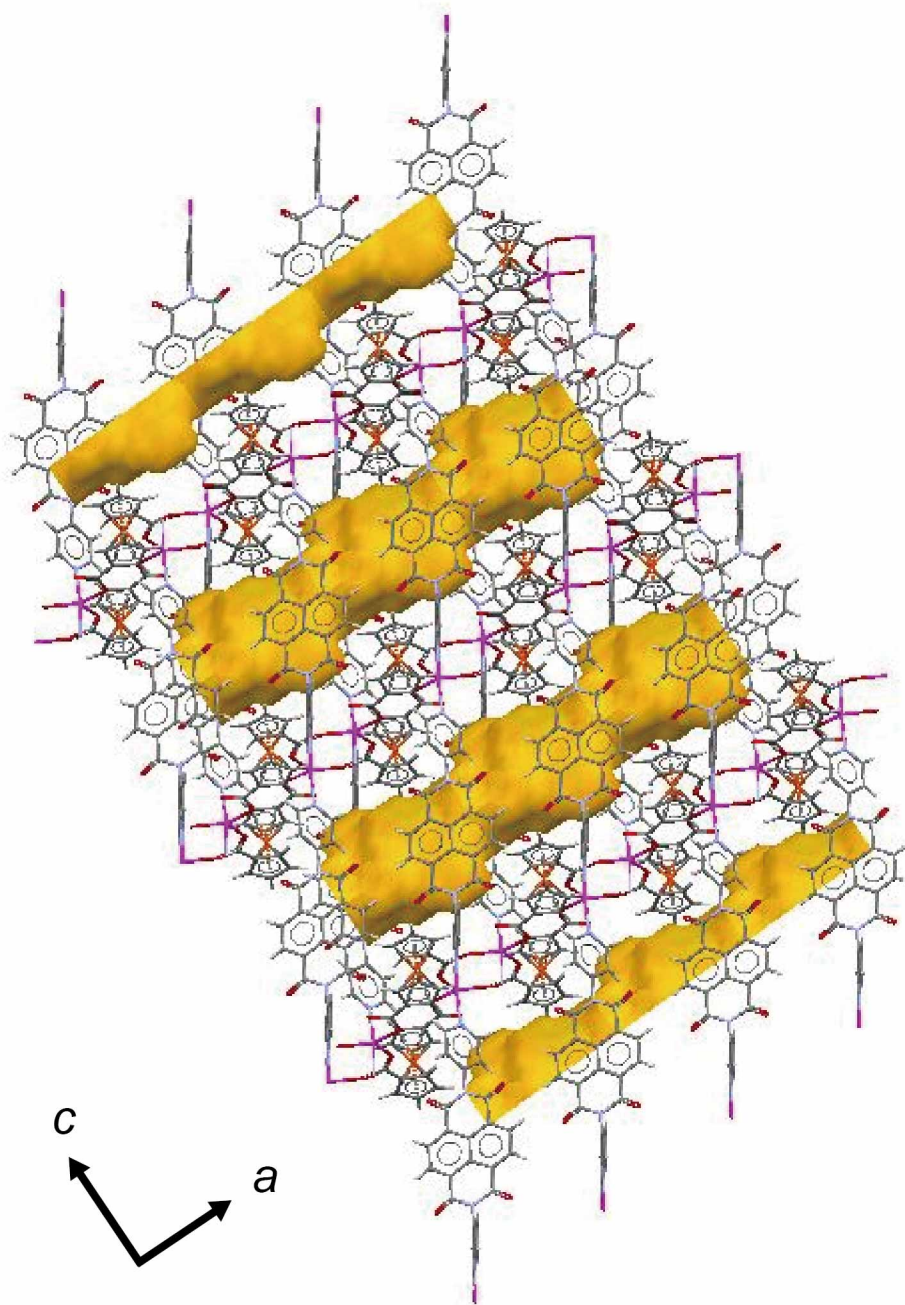


Fig. S3 Contact surface with a probe radius of 1.2 Å emphasizing the undulating 1D channels (gold) of **3**.

5. Thermogravimetric analysis of **1**, **2** and **3**

Thermogravimetric (TG) analysis were performed using a Rigaku Thermo plus TG 8120 apparatus in the temperature range between 298 and 773 K in a N₂ atmosphere and at a heating rate of 10 Kmin⁻¹. The first weight loss from the **1**, **2** and **3** \square solvents, 9.6, 8.4 and 6.5 wt% respectively, corresponded to the loss of solvent molecules. Although **1** was decomposed around 250 °C, **2** and **3** were stable up to 350 °C.

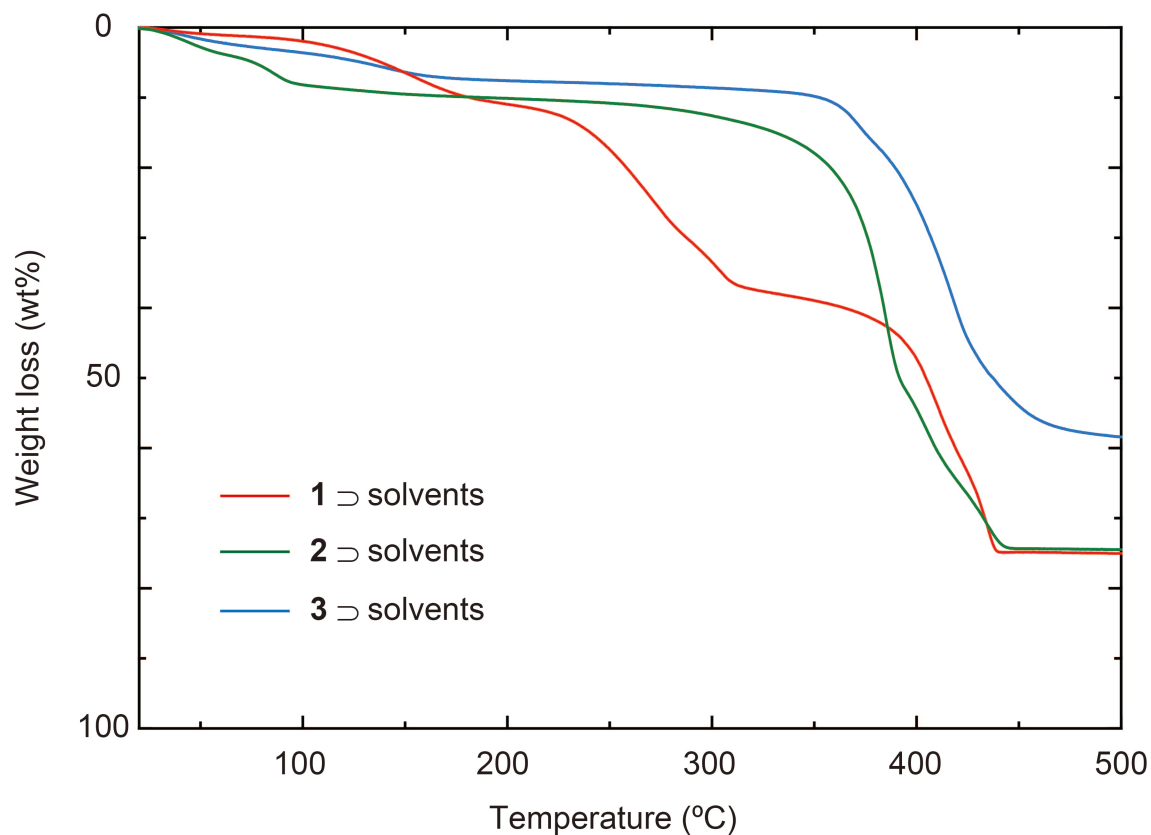


Fig. S4 TG analysis showing the weight loss in **1**, **2** and **3** \square solvents. The observed weight loss corresponds to the weight of solvent molecules.

6. XRD of bulk powder crystals of **1**

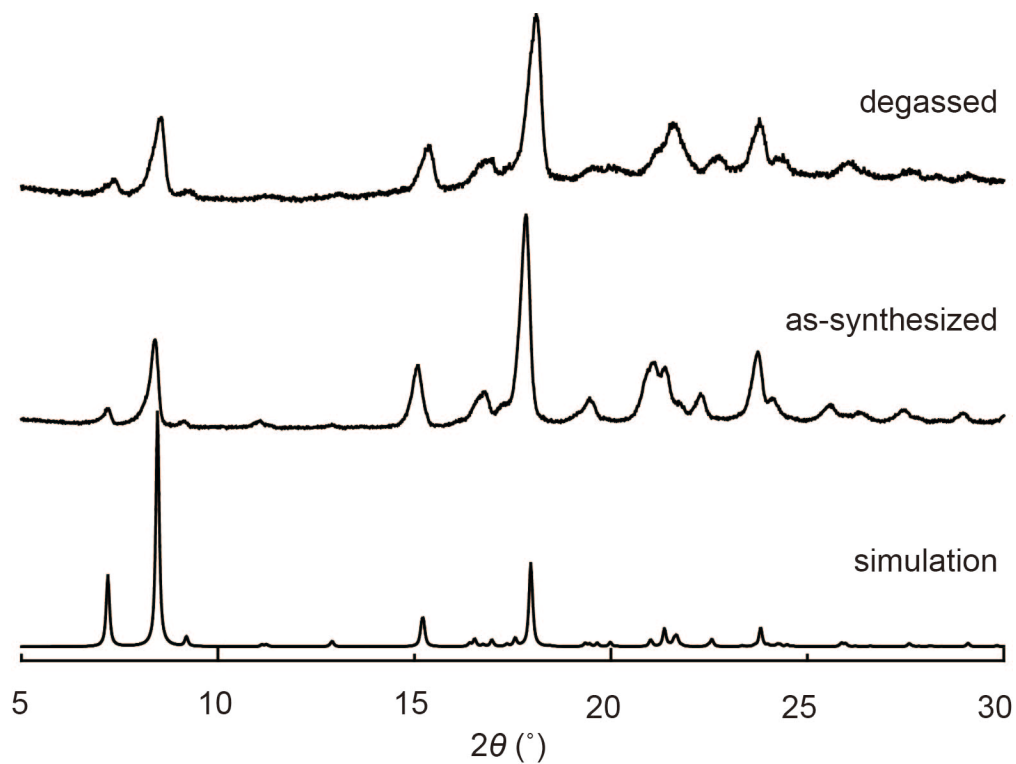


Fig. S5 Powder X-ray diffraction patterns of as-synthesized, degassed, and simulated **1**.

7. XRD of bulk powder crystals of **2**

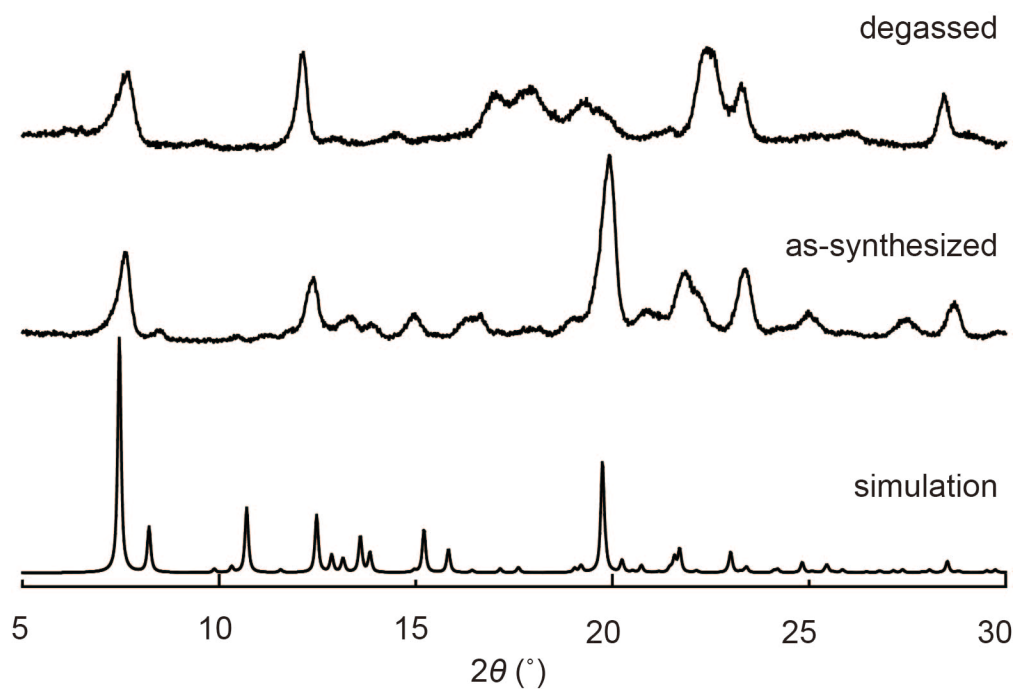


Fig. S6 Powder X-ray diffraction patterns of as-synthesized, degassed, and simulated **2**.

8. XRD of bulk powder crystals of 3

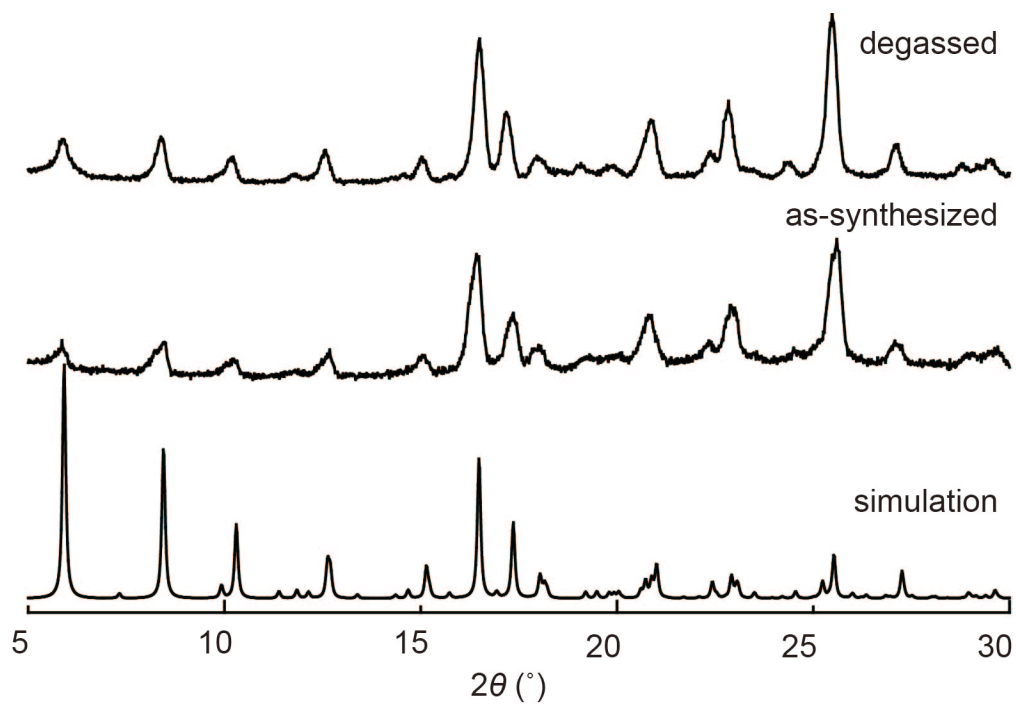


Fig. S7 Powder X-ray diffraction patterns of as-synthesized, degassed, and simulated **2**.

9. Adsorption measurements of **1**

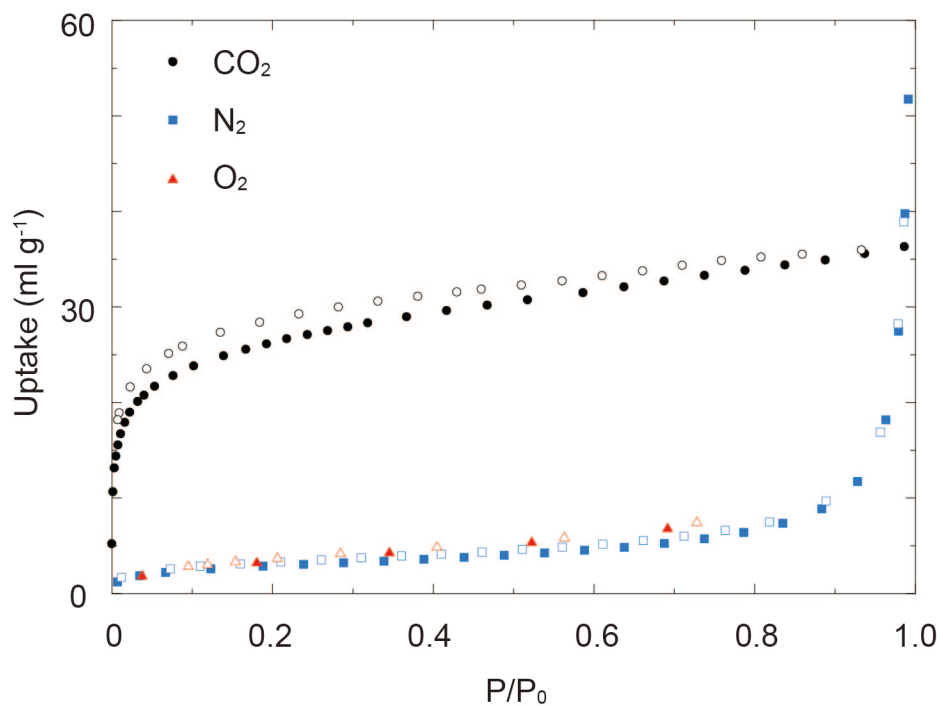


Fig. S8 Adsorption isotherms of gas molecules for **1**. Closed and open symbols show adsorption and desorption, respectively

10. Adsorption measurements of **2**

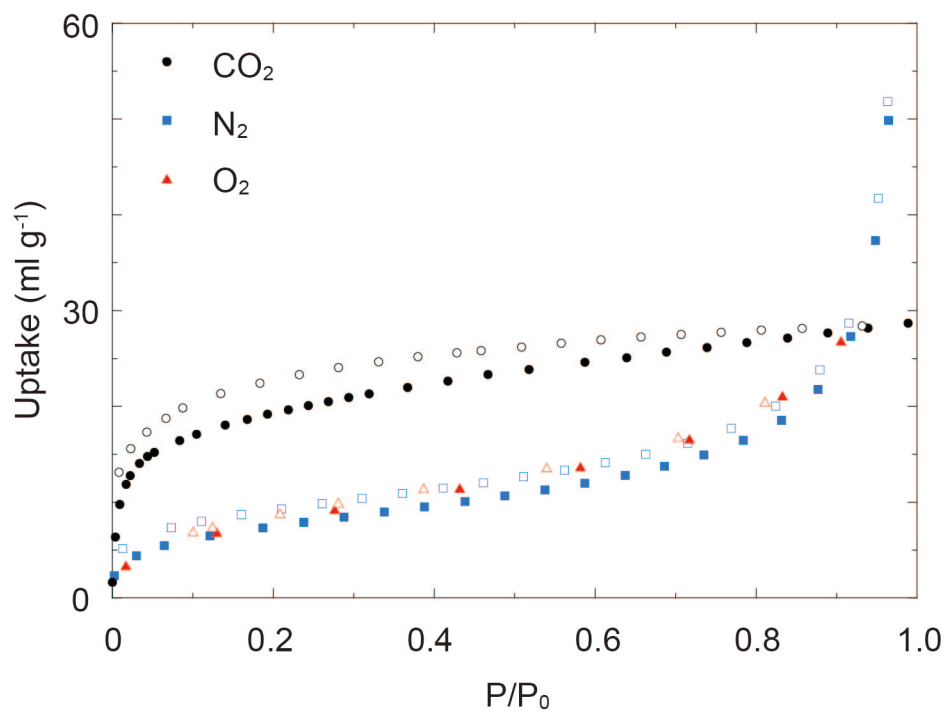


Fig. S9 Adsorption isotherms of gas molecules for **2**. Closed and open symbols show adsorption and desorption, respectively

11. Adsorption measurements of **3**

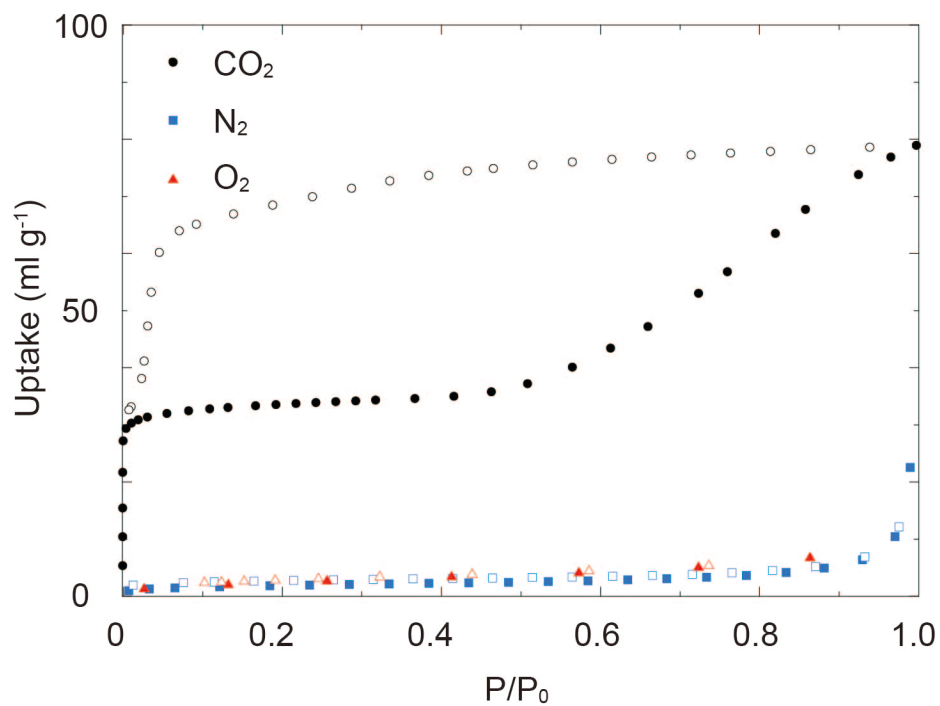


Fig. S10 Adsorption isotherms of gas molecules for **3**. Closed and open symbols show adsorption and desorption, respectively

12. XRD of Crystals of 2 on Au electrodes

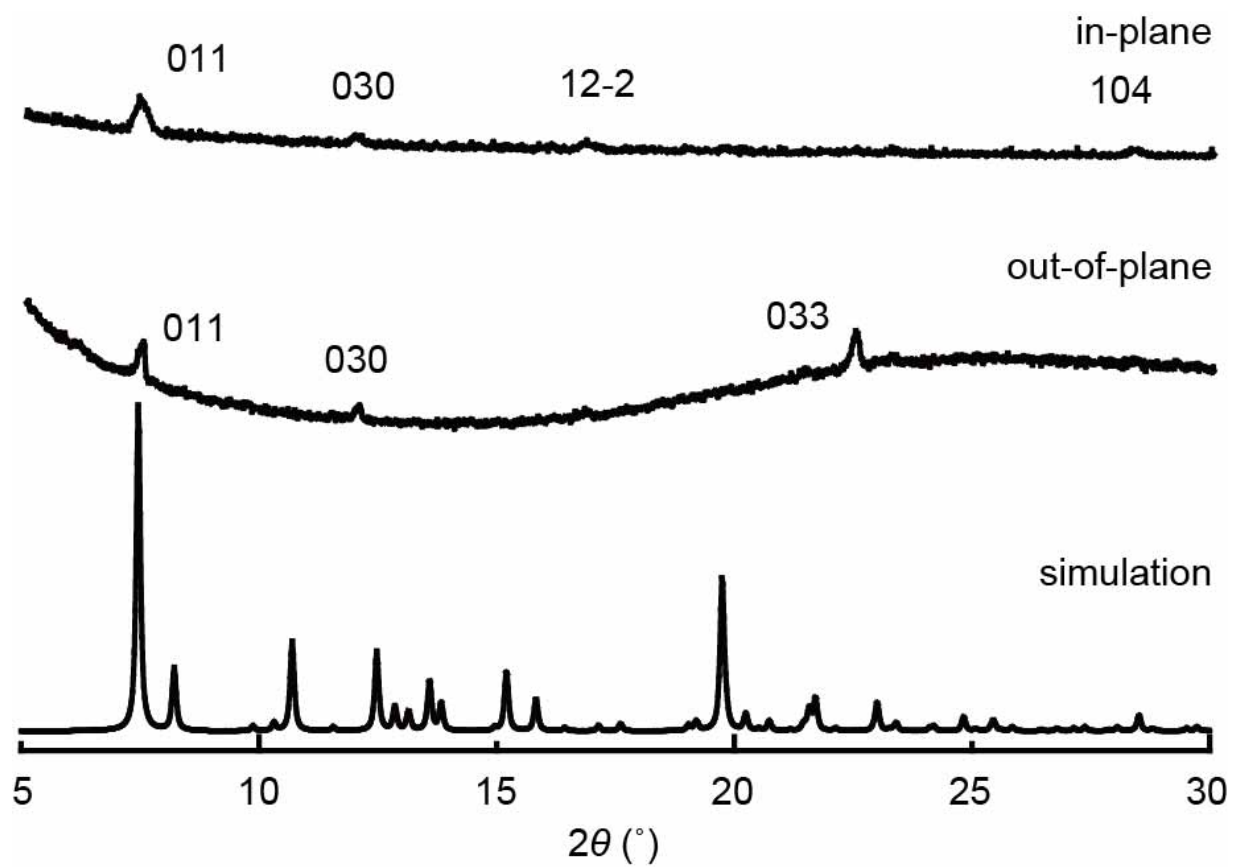


Fig. S11 XRD patterns of in-plane diffraction, out-of-plane diffraction, and simulation of 2.

13. XRD of Crystals of 3 on Au electrodes

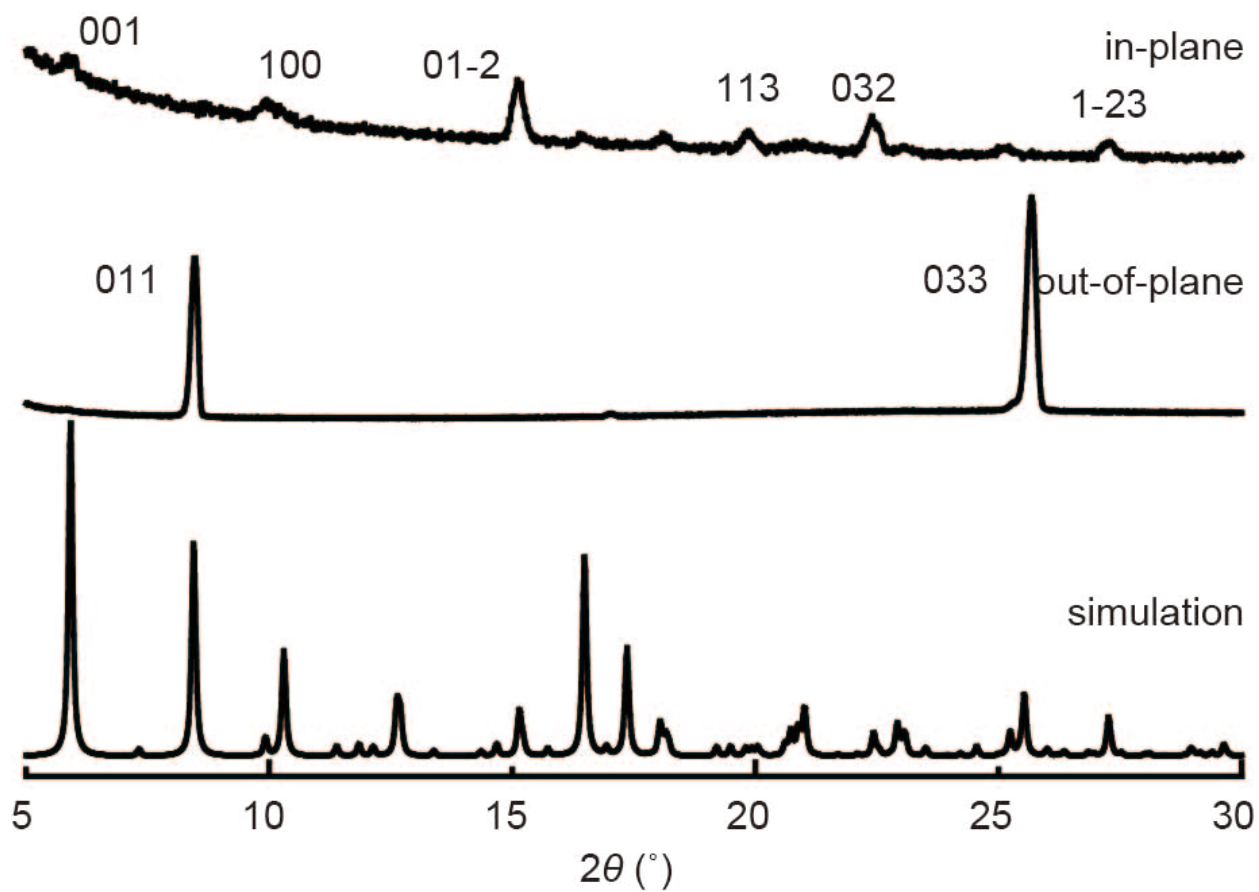


Fig. S10 XRD patterns of in-plane diffraction, out-of-plane diffraction, and simulation of 3

14. IR-RAS measurement of Crystals of **1** on an Au electrode

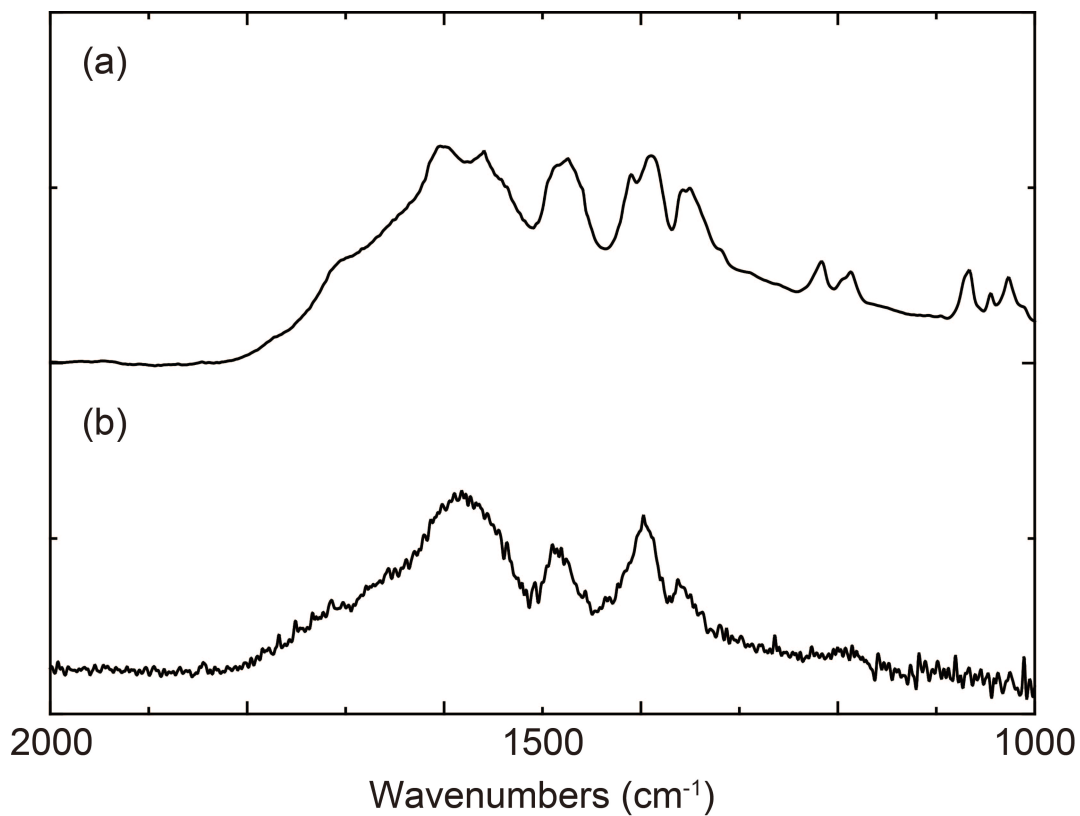


Fig. S13 (a) Reflectance IR spectrum of bulk crystals of **1**, (b) IR-RAS spectrum of **1** on Au substrate

Reference

S1 P. H. Dinolfo, M. E. Williams, C. L. Stern, J. T. Hupp, *J. Am. Chem. Soc.*, **2004**, 126, 12989.

S2 K. Biradha and M. Fujita, *J. Chem. Soc., Dalton Trans.*, **2000**, 3805.